LEVEL II 12

ADDITIONAL RESULTS OF A STUDY OF UNSTEADY AIRFOIL SURFACE PRESSURES AND TURBULENT BOUNDARY LAYERS

MASSACHUSETTS INSTITUTE OF TECHNOLOGY
AEROPHYSICS LABORATORY

by

Peter F. Lorber

and Eugene E. Covert

Massachusetts Institute of Technology
Department of Aeronautics and Astronautics
Cambridge, Ma 02139

ANNUAL ~~FINAL~~ REPORT

TR 212

November, 1981

Distribution
Unlimited

Approved for public release; distribution unlimited.

Grant No. AFOSR-80-0282

UNCLASSIFIED

SECURITY CLASSIFICATION OF THIS PAGE (When Data Entered)

REPORT DOCUMENTATION PAGE		READ INSTRUCTIONS BEFORE COMPLETING FORM
1. REPORT NUMBER AFOSR-TR- 81-0848	2. GOVT ACCESSION NO. AD-A108 978	3. RECIPIENT'S CATALOG NUMBER
4. TITLE (and Subtitle) ADDITIONAL RESULTS OF A STUDY OF UNSTEADY AIRFOIL SURFACE PRESSURES AND TURBULENT BOUNDARY LAYERS		5. TYPE OF REPORT & PERIOD COVERED ANNUAL 1 SEP 80 - 31 Aug 81 6. PERFORMING ORG. REPORT NUMBER TR-212
7. AUTHOR(s) EUGENE E COVERT PETER F LORBER		8. CONTRACT OR GRANT NUMBER(s) AFOSR-80-0282
9. PERFORMING ORGANIZATION NAME AND ADDRESS MASSACHUSETTS INSTITUTE OF TECHNOLOGY DEPT OF AERONAUTICS & ASTRONAUTICS CAMBRIDGE, MA 02139		10. PROGRAM ELEMENT, PROJECT, TASK AREA & WORK UNIT NUMBERS 61102F 2307/A2
11. CONTROLLING OFFICE NAME AND ADDRESS AIR FORCE OFFICE OF SCIENTIFIC RESEARCH/NA BOLLING AIR FORCE BASE, DC 20332		12. REPORT DATE NOV 81 13. NUMBER OF PAGES 36
14. MONITORING AGENCY NAME & ADDRESS(if different from Controlling Office)		15. SECURITY CLASS. (of this report) UNCLASSIFIED 15a. DECLASSIFICATION/DOWNGRADING SCHEDULE

16. DISTRIBUTION STATEMENT (of this Report)

Approved for public release; distribution unlimited.

17. DISTRIBUTION STATEMENT (of the abstract entered in Block 20, if different from Report)

18. SUPPLEMENTARY NOTES

19. KEY WORDS (Continue on reverse side if necessary and identify by block number)

GROUND TESTING
WIND TUNNEL
UNSTEADY FLOW
UNSTEADY BOUNDARY LAYER

20. ABSTRACT (Continue on reverse side if necessary and identify by block number)

Unsteady pressure coefficients measured on an N.A.C.A. 0012 airfoil at geometric angles of attack of 0 and 10 degrees, Reynolds numbers of 700,000 and 1,000,000 and in the reduced frequency range of 0.5 to 6.4 (based upon the half chord) are presented. For simplicity the data are represented in terms of mean and unsteady pressure coefficients, which has both a magnitude and a phase. Primary conclusions are: 1) The difference pressures approach zero at the trailing edge. This corresponds to satisfying one statement of the Kutta condition. 2) Superposition

DD FORM 1 JAN 73 1473 EDITION OF 1 NOV 65 IS OBSOLETE 220003 UNCLASSIFIED

A

SECURITY CLASSIFICATION OF THIS PAGE (When Data Entered)

of the unsteady processes in the steady flow seems accurate and valid up to reduced frequencies of 2. 3) For this airfoil with 16° trailing edge angle the effects of viscosity seem to be most prominent in the last 10 percent of the airfoil where the phase lags are much larger than those predicted by the linear theory.

Technical Summary

An annual report for an ongoing research project presents certain challenges if the primary effort is experimental because of the vagaries of carrying out an experiment. For the most part vagaries usually result in stretching out of the schedule. Thus it is difficult to produce a tidy, cogent annual report.

This year a somewhat different approach will be used. The research naturally splits into two parts. The first part is the unsteady pressure distribution of an NACA 0012 airfoil. These characteristics have been measured at low Mach numbers, in the Reynolds Number range of 0.3 to 1.0 million, in the reduced frequency range of 0.5 to 6.4, and at geometric angles of attack of 0 and 10 degrees. All in all, this constitutes a large body of data. Proper management of this data has required considerable software development. In order to efficiently manipulate this data using the computer, some of the data collected last year was retaken, since it was not in a form compatible with the computer. Because of a delay in the wind tunnel schedule, the 10^{o} upwash data is not complete, which hampers calculations, and no data has been taken above the stall, as planned.

The second part is to measure unsteady boundary layer characteristics and compare that data with calculations based on the unsteady pressure data referred to above. We are

particularly interested in the change in characteristics as separation is approached. Because of scheduling problems in the wind tunnel, only tangential velocity profiles have been recorded.

Hence, this report will concentrate on the recent unsteady airfoil measurements and its implications and relate these to earlier results. A report on the Boundary Layer Characteristics will be prepared subsequently.

Physical Arrangement

Figure 1 shows the wind tunnel section, as used for unsteady airfoil pressure studies. The arrangement of airfoil, sidewalls and rotating elliptic cylinder have been described in References 1, 2 and 3. A summary is given as Appendix A.

Data Acquisition

The data acquisition system used to obtain the present results is shown in Figure 2. Pulses produced when the elliptic cylinder major axis is parallel to the freestream ($\theta = 0$) trigger and synchronize data taking. Transducer voltages are then sampled at rates computed so as to fit the desired number of samples into each rotation period. This procedure compensates for any drift in the cylinder period. Between 64 and 512 readings are taken each period, limited by the number of simultaneous inputs and by the length of the period. The present

system allows a maximum of 8 channels to be sampled at up to 17 kHz, divided by the number of channels.

Ensemble averaging is performed by averaging the set of readings for each period over a number of periods that ranges from 50 to 100 for pressure data to 200 to 5000 periods for low amplitude turbulent velocities. These averages are converted to coefficient form and displayed graphically to check system operation and to allow further study of unusual results. Ensemble averages are stored on floppy discs for later processing.

Data Processing and Analysis

Following completion of a test, ensemble averaged pressure and velocity data may be analyzed in several ways. First, the nondimensionalized ensemble averages may be plotted against time and another parameter such as chordwise position or height in the boundary layer in a "three-dimensional" graph. This technique is useful to illustrate the general character of the data, revealing features that may be overlooked in more specific analysis procedures.

Second, the ensemble averages may be Fast-Fourier transformed, obtaining amplitudes and phase lags for the harmonics of the cylinder rotation frequency. Harmonics up to 10 were commonly examined; however, only the first few had amplitudes high enough to be of interest.

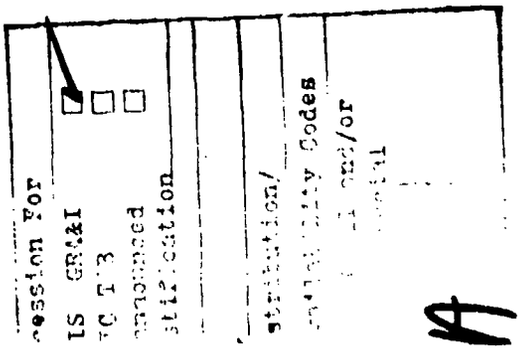

Third, ensemble averages at several positions may be operated upon to produce new parameters describing the more global situation. For example, velocity profiles were integrated to find unsteady displacement and momentum thicknesses and the shape parameter, H. Pressure distributions were integrated over the airfoil surface to determine unsteady section lift and pressure drag coefficients, and differentiated to give the pressure gradient. The parameters could then be Fourier transformed into amplitudes and phase lags.

Fourth, theoretical models may be applied to attempt to link various sets of data. A modification of Theodorsen's unsteady thin airfoil theory (References 2, 4, 5) was used to operate on the unsteady upwash distributions to produce a prediction for the airfoil difference pressure distribution and lift coefficient.

During all of these analysis procedures, there are many opportunities to produce graphics terminal plots and to print out the distributions, transforms, other plots deemed instructive in understanding the physical processes under study.

Test Conditions

The current test series acquired data for two geometric angles of attack, (α), 0 and 10 degrees. At zero degrees, airfoil pressures were measured for Reynolds numbers of .7 and 1.0×10^6 and reduced frequencies of 0.5, 1.0, 1.5, 2.0, 4.0 (3.9 for $R_e = .7 \times 10^6$) and 6.4 (5.1 for $R_e = 1 \times 10^6$). Steady pressures were measured for elliptic cylinder orientations of

θ = 0, 45, 90 and 135 degrees. Unsteady boundary layer tangential velocity profiles were obtained at the chordwise location x/c = 0.94 and $R_e = .7 \times 10^6$ for k = 0.5, 1.0, 2.0 and 6.4, and at x/c = 0.96, $R_e = .7 \times 10^6$ and k = 1.0.

For airfoil at 10 degrees, pressure data was taken for $R_e = .7$ and 1.0×10^6 at reduced frequencies of 0.5, 1.0, 2.0, 4.0 (3.9) and 6.4 (5.1), and for steady elliptic cylinder orientations of θ = 0, 45, 90, 135 degrees. Boundary layer profiles at x/c = .94 and $R_e = .7 \times 10^6$, for k = 0.5, 1.0, 2.0, 3.9 and 6.4 were then measured.

Although data acquisition programming and experimental apparatus were prepared for additional studies of upwash, pressure, boundary layer velocities and Reynold's stresses at increased angles of attack and decreased separation between trailing edge and elliptic cylinder, delays in the availability of the wind tunnel made it impossible to perform these tests in the current period.

Surface Pressure Results

Airfoil surface pressures were first measured at zero angle of attack with no elliptical cylinder present, and compared with the accepted pressure coefficient distributions for the NACA 0012 (Reference 6). This comparison is shown as Figure 3. The acceptable agreement validates the airfoil contour and the technique of measuring dynamic pressure with a pilot-static probe located above the airfoil and between the sidewalls, as shown in Figure 1.

Figures 4 and 5 show the distribution of the mean, or time average pressure coefficient for airfoil angles of attack of 0 and 10 degrees, respectively. Data are given for a Reynold's number of 10^6 for reduced frequencies ranging from 0.5 to 5.1, as indicated by the data symbols. The major effects of the increasing reduced frequency on the mean pressure distribution are an increase in the pressure difference (upper-lower) due to the increased circulation and a lowering of the pressure coefficients near the trailing edge. On the average no separation was indicated by these data.

Figure 6 is a plot of the ensemble averaged upper surface pressure coefficient at reduced frequency = 6.4, zero angle of attack, and $R_e = .7 \times 10^6$. The horizontal axis represents time, with 720 degrees of phase corresponding to one elliptical cylinder rotation period. The third, slanted axis is for position along the airfoil chord. The data show the smooth variations in both means and amplitudes that were typically present, with the increased amplitudes near the trailing edge being apparent.

Figure 7 is a similar plot of the difference pressure coefficient at reduced frequency 1.0. The smooth decrease in amplitudes from the leading edge to the trailing edge can be seen, together with the phase shifts near the leading and trailing edges. Figure 8 shows the amplitude of the fundamental harmonic (twice the cylinder frequency). For K = 3.9 and

alpha = 0, upper surface, lower surface, and difference amplitudes are given. The trend of the difference pressure toward 0 at the trailing edge is apparent. Figure 9 presents the phase lag distributions for the same conditions. Note the increased phase lags of the difference pressure at the edges, and the decreased phase lag of the upper surface pressure at the leading edge. The difference pressure phase behavior is discussed below, while the phase behavior of the upper surface is covered in more detail, but still not completely explained in References 1, 2, 3).

As discussed at length in References 2 and 3, the measured unsteady difference pressure distributions were compared to predictions made by applying unsteady incompressible thin airfoil theory to the measured unsteady upwash distributions. Typical results are shown in the next three figures. Figure 10 shows the good agreement between measured and predicted mean difference pressures at k = 6.4 and alpha = 0 degrees. Although a correction was applied to remove the singularity at the leading edge (Reference 7), the prediction still overestimated the measured values in that region.

Figure 11 gives results for the fundamental harmonic at k = 2.0. Qualitative agreement is seen, but predicted amplitudes were much higher than the pressure requirements. Figure 12 shows the phase lag results for this case. The agreement is acceptable over the forward 80% of the chord, with major differences appearing near the trailing edge. The trailing edge behavior is discussed at greater length below and in Reference 8.

Figure 13 shows the mean difference pressure near the trailing edge, normalized by the value at x/c = 0.75. All airfoil angle of attack and reduced frequency combinations at R_e = 700,000 are included. A typical prediction, similarly normalized, is also shown. Apart from the functional dependence of k on the individual distributions, the most obvious feature is the difference in the manner in which the distributions approach zero at the trailing edge. The prediction has higher curvature, approaching zero very rapidly over the last few percent of chord. This difference is presumably due to the finite trailing edge angle and to viscous effects near the trailing edge, neither of which are included in the theory.

Figure 14 presents the fundamental harmonic of the difference pressure for the same cases, similarly normalized. The effects of k on the detailed pressure distributions is somewhat greater than in the mean pressure distribution but each distribution appears to be approaching a value of zero at the trailing edge. The very rapid drop to zero of the prediction is even more pronounced for this unsteady portion than for the mean. Measured values again approach zero more gradually.

Finally, Figure 15 gives phase lag data for these frequency Reynold's number and angle of attack conditions. All distributions are normalized by the phase lag at x/c = 0.75. The differences in behavior seen in Figure 12 are apparent to varying degrees for all cases. Trailing edge phase lag measurements were generally larger for higher frequencies and higher

angles of attack, and were relatively independent of Reynold's number. The predicted phase lag distributions for k = 1.0 and k = 6.4 at zero angle of attack and $R_e = .7 \times 10^6$ are also shown in Figure 15 for comparison. In the region .9 < x/c < .97 both calculated and measured phase lags increased with reduced frequency. The calculations, however, predicted a smaller increase, and in fact, for x/c > .98, a sharp drop to a phase lag of -90° with respect to the phase of the upwash is predicted. This drop is not seen in the measurements. The agreement for x/c < .9 is encouraging, and would seem to indicate that at least some of the unsteady effects are being correctly modelled. The increased phase lags with increased angle of attack may be due to the thicker boundary layers, representing a greater departure from the cusped edge, inviscid flow postulated by the theoretical model.

As discussed above, the measured unsteady surface pressure distributions could be integrated using the trapezoidal rule along the surface of the airfoil and Fourier transformed to produce harmonic amplitudes and phase lags for the lift and pressure drag. Figure 16 shows the unsteady lift magnitude for the fundamental harmonic plotted against the reduced frequency. For frequencies of 2.0 and below, the results seen to be relatively independent of Raynold's number and angle of attack. This suggests superposition of the unsteady upwash increment onto steady properties due to thickness, angle of attack and mean upwash is valid. For higher reduced frequencies the differences increased, in particular the Reynold's number seemed to play an important role above k = 4.

Predicted unsteady lift amplitudes for zero angle of attack are also given on Figure 16. Qualitative agreement between measurement and calculation is seen at higher reduced frequencies and including the reduction in amplitudes between $k = 1$ and $k = 4$. As would be expected from the pressure distribution in Figure 14, predicted lift amplitudes are significantly larger than the measured values.

Figure 17 shows the phase lag for the same unsteady lift conditions. The phase lag is seen to be relatively independent of Reynold's number and angle of attack, with all data being within approximately five degrees of a common curve of variable reduced frequency. Predicted phase lags for angle of attack are also presented. Qualitative agreement was noted regarding low values for $k < 2$, with decreasing phase lag as the reduced frequency increased. The difference with Reynold's number of the predictions was probably due to uncertainties in the analog system used to collect the upwash data and to the requirement to use an averaged phase valve for the entire upwash distribution. This is discussed at greater length in Reference 2.

Conclusions/Accomplishments

For the present experimental situation:

1) Unsteady difference pressures appear to approach a value of zero at the airfoil trailing edge, for reduced frequencies up to 6.4 and at airfoil angle of attack up to 10 degrees ($\bar{c}_L = 1.2$).

2) Near the airfoil trailing edge, mean and unsteady difference pressure are each characterized by similar normalized distributions. These distributions approach zero more gradually than predicted by unsteady thin airfoil theory, based upon measured upwash distributions.

3) Unsteady difference pressure phase behavior is not well modelled near the airfoil trailing edge by the thin airfoil theory. It seems likely the phase is affected by a finite trailing edge angle and a significant boundary layer.

4) Unsteady lift amplitudes and phase behavior may be qualitatively predicted by unsteady thin airfoil theory, but amplitudes tend to be less than predicted.

Appendix A

Experimental Apparatus and Procedure

The experimental measurements were made at M.I.T.'s Wright Brothers Memorial Wind Tunnel, a low speed facility having a 2.3 m x 3.0 m elliptical test section (Figure 1). The NACA 0012 airfoil section used had a 20 cm chord, which, together with the tested free stream velocities of 20 and 30 mps, gave Reynold's numbers of 7×10^5 and 1×10^6. Vertical sidewalls spanned the full height of the tunnel, and were 2.4 airfoil chords long. The sidewalls diverged downstream to minimize pressure gradients. Joints between sidewall and airfoil were sealed to prevent secondary flows. Two dimensionality was confirmed by measuring steady flat plate boundary layer profiles and comparing these profiles with standard results (9). The airfoil steady angle of attack was set by rotation about the trailing edge.

The rotating elliptic cylinder had major axes of 6.50x 13.77 cm, and had its axis at x/c = 1.175, y/c = -0.276. It could be spun at up to 3300 rpm. A pulse produced each revolution provided a phase reference to synchronize data acquisition. The cylinder surface was roughened to delay separation and increase repeatability. Fundamental reduced frequencies, $k = \omega c/2U_\infty$, obtained ranged from 0.5 to 6.4.

The instrumentation may be conveniently divided into three functional categories. First, a cross hot wire was used to

measure flow velocities induced along the airfoil chord line by the elliptic cylinder, with no airfoil in the wind tunnel. Second, pressure taps located along the airfoil surfaces determined unsteady pressure distributions. Third, a single wire hot-wire probe was used to get tangential velocity profiles in the airfoil boundary layer.

The induced flow velocity measuring system and the results obtained are discussed at length in References 2 and 3. In brief, the mean and the ensemble (phase locked) average of the unsteady upwash distributions were measured from $x/c = 0$ to $x/c = 1.1$. Distributions were found to depend primarily upon reduced frequency, over the Reynold's number range of .3 to 1.0×10^6, with maximum amplitudes, both mean and unsteady, occuring near the trailing edge position. Means increased with reduced frequency, due to the increased circulation generated by the cylinder's rotation. Unsteady amplitudes decreased above $k = 1$ because of increased acceleration required by the fluid. For some frequencies the expected symmetry between cylinder half-rotation periods was significantly distorted. Such frequencies were avoided, as described in References 2 and 3.

Seventeen pressure taps were located on each airfoil surface, from $x/c = 0.005$ to $x/c = 0.98$. They were connected to upper and lower surface Scanivalves using 25 cm tubing, fitted with yarn inserts to avoid resonance problems in the frequency band of interest, 0 to 600 Hz. Pressures were measured using Setra model 237 capacitive transducers, with a range of

$\pm$ 3800 Nt/m^2 ($\pm$ 0.5 psi). The amplitude and phase calibration procedure is described in Reference 3. The results are shown in Figures A-1 and A-2. The phase calibration of Figure A-2 was subtracted from the experimental results.

Airfoil boundary layer velocity profiles were found by moving a normal wire constant temperature hot wire anemometer perpendicular to the surface. The probe was capable of being moved in increments of 0.0025 cm or greater, to within 0.013 cm of the surface. Typical boundary layer thicknesses (u = 0.995 Ue) present at the measurement station of x/c = 0.94 ranged from 1.2 to 2.5 cm, so that the spatial resolution was sufficient. A linear potentiometer was used to determine probe heights. The probe was frequently moved outside of the boundary layer during each profile to check for thermal drift.

REFERENCES

1. Lorber, P F and E E Covert, "Preliminary results of a study of unsteady airfoil surface pressures and turbulent boundary layers", M.I.T. Aerophysics Lab. TR 210, December, 1980; also AFOSR

2. Lorber, P F, "Unsteady airfoil pressures induced by perturbation of the trailing edge flow", S.M. Thesis, Aeronautics and Astronautics Department, M.I.T., February, 1981.

3. Covert, E E and P F Lorber, "Unsteady airfoil pressures produced by periodic aerodynamic interference", submitted to AIAA Journal.

4. Theodorsen, T, "General theory of aerodynamic instability and the mechanics of flutter", N.A.C.A. Report 496, 1934.

5. Bisplinghoff, R L, H Ashley, and R L Halfman, "Aeroelasticity", Addison-Wesley Publishing Co., Inc., Cambridge, Ma, 1955, pp 251-281.

6. Abbott, I H and A E von Doenhoff, "Theory of wing sections", Dover Publications, Inc., New York, 1959, p 321.

7. Van Dyke, M, "Perturbation methods in fluid mechanics", Academic Press, Inc., New York, 1964, pp 59-61.

8. Covert, E E and P F Lorber, "On the Kutta condition in unsteady flow", submitted to the Journal of Fluid Mechanics.

9. Kanevsky, A R, and E E Covert, "Preliminary experiment design to support a feasibility demonstration, Interim Report", AFOSR-TR-0902, 1978.

Status of Research

With the exception of the slip in the tunnel, which was due to a fatigue failure in the tunnel drive mechanisms, the work is proceeding reasonably well. The results to date have indicated the simple theories, like Theodorsen's have a much greater range than originally expected (k = 2). The same may be said for the non-singular behavior of the pressure and the trailing edge (the Kutta condition seems to represent the physics of the outer flow) up to reduced frequencies (k) of 6.4. The data at a geometric angle of attack of 10 degrees also seems to support these conclusions, although the detail analysis awaits measurement of the upwash distribution.

Although not discussed in this report the same sort of remarks apply for the boundary layer studies and measurements and for the shear gauge development.

Culmulative Publications

1. Lorber, P F and E E Covert, "Unsteady airfoil pressures produced by periodic aerodynamic interference", submitted to AIAA Journal (February, 1981).
2. Lorber, P F and E E Covert, "On the Kutta condition in unsteady flow (submitted to Journal of Fluid Mechanics".

Professional Personnel

The following people have made important contributions to this project in the last year:

1.	Professor E E Covert	Principal Investigator
2.	P F Lorber	Research Assistant
3.	R Lee	Research Assistant
4.	Dr C W Haldeman	Principal Research Associate
5.	Mr Paul Bauer	Research Engineer

In February, 1981, Mr Lorber was awarded the degree of S.M. in Aeronautics and Astronautics from M.I.T. Mr. Lorber's thesis was prepared under this grant. This thesis was entitled "Unsteady Airfoil Pressures Induced by Perturbation of the Trailing Edge Flo . .

Interactions

The primary interactions fall into two classes. First, wind tunnel procedures have been discussed with a group of wind tunnel engineers (the Supersonic Tunnel Association (October, 1980)). Informal discussions about the data and its usefulness have been held with Dr McCrosky of the Army Mobility Laboratory, Ames Research Center, California and with Dr S K F Karlsson of Brown University in June, 1981.

Professor Covert was invited by Dr Hearth, Director of NASA Langley Research Center, to be the Chairman of a Peer Group Review Committee for the Unsteady Aerodynamics Branch at that Center.

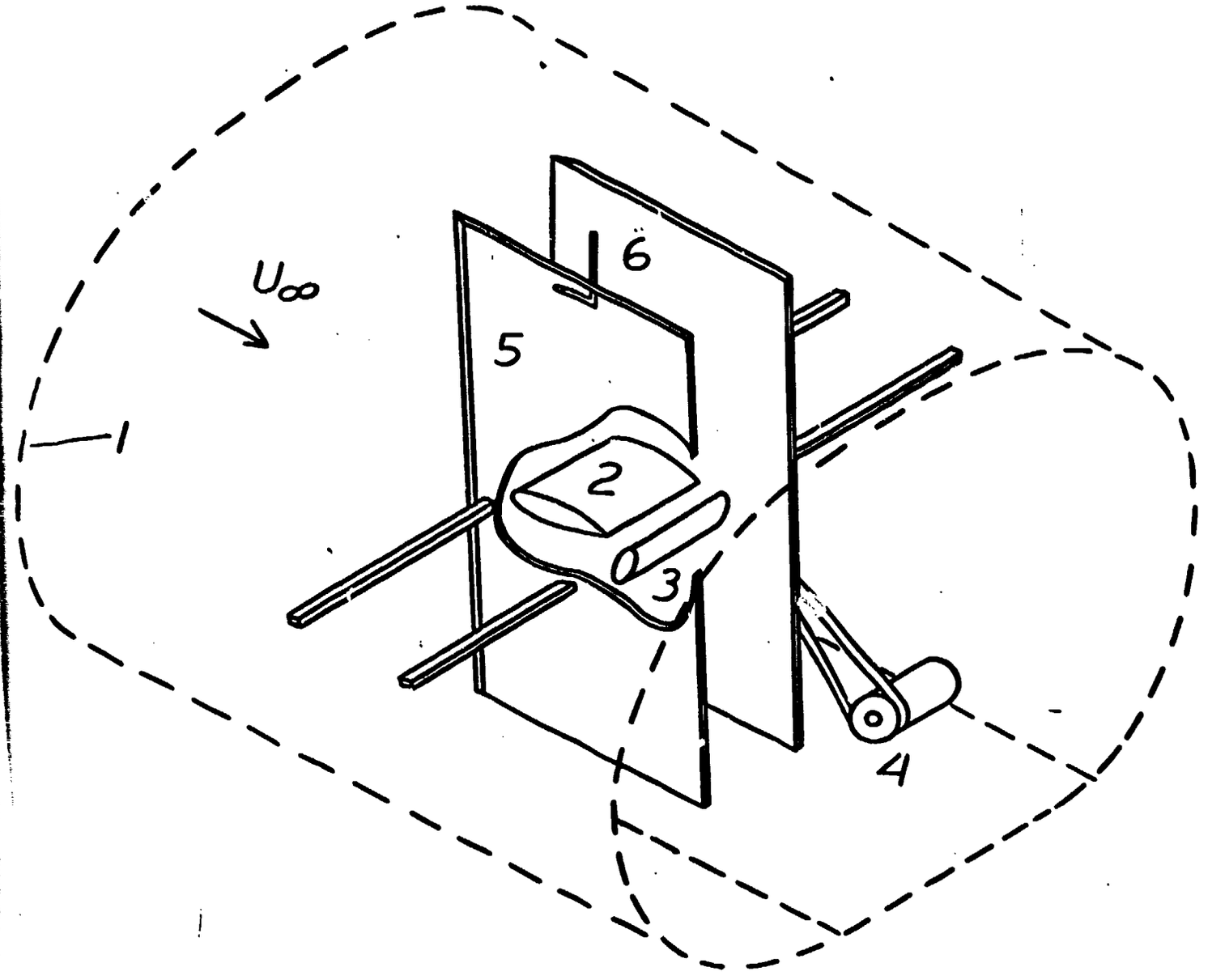

FIGURE 1

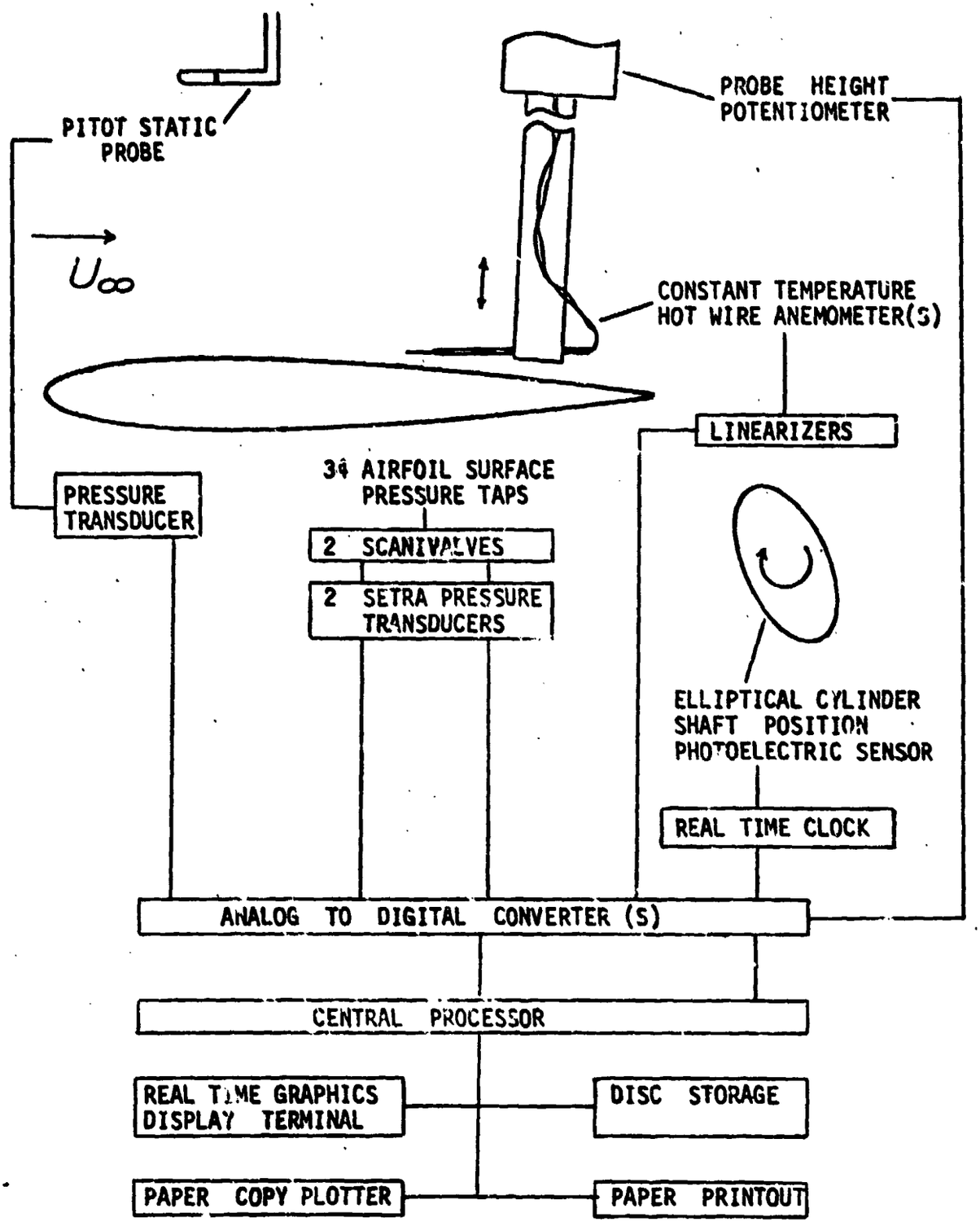
PITOT STATIC PROBE
PROBE HEIGHT POTENTIOMETER
U_∞
CONSTANT TEMPERATURE HOT WIRE ANEMOMETER(S)
LINEARIZERS
34 AIRFOIL SURFACE PRESSURE TAPS
PRESSURE TRANSDUCER
2 SCANIVALVES
2 SETRA PRESSURE TRANSDUCERS
ELLIPTICAL CYLINDER SHAFT POSITION PHOTOELECTRIC SENSOR
REAL TIME CLOCK
ANALOG TO DIGITAL CONVERTER (S)
CENTRAL PROCESSOR
REAL TIME GRAPHICS DISPLAY TERMINAL
DISC STORAGE
PAPER COPY PLOTTER
PAPER PRINTOUT

FIGURE 2

2 L

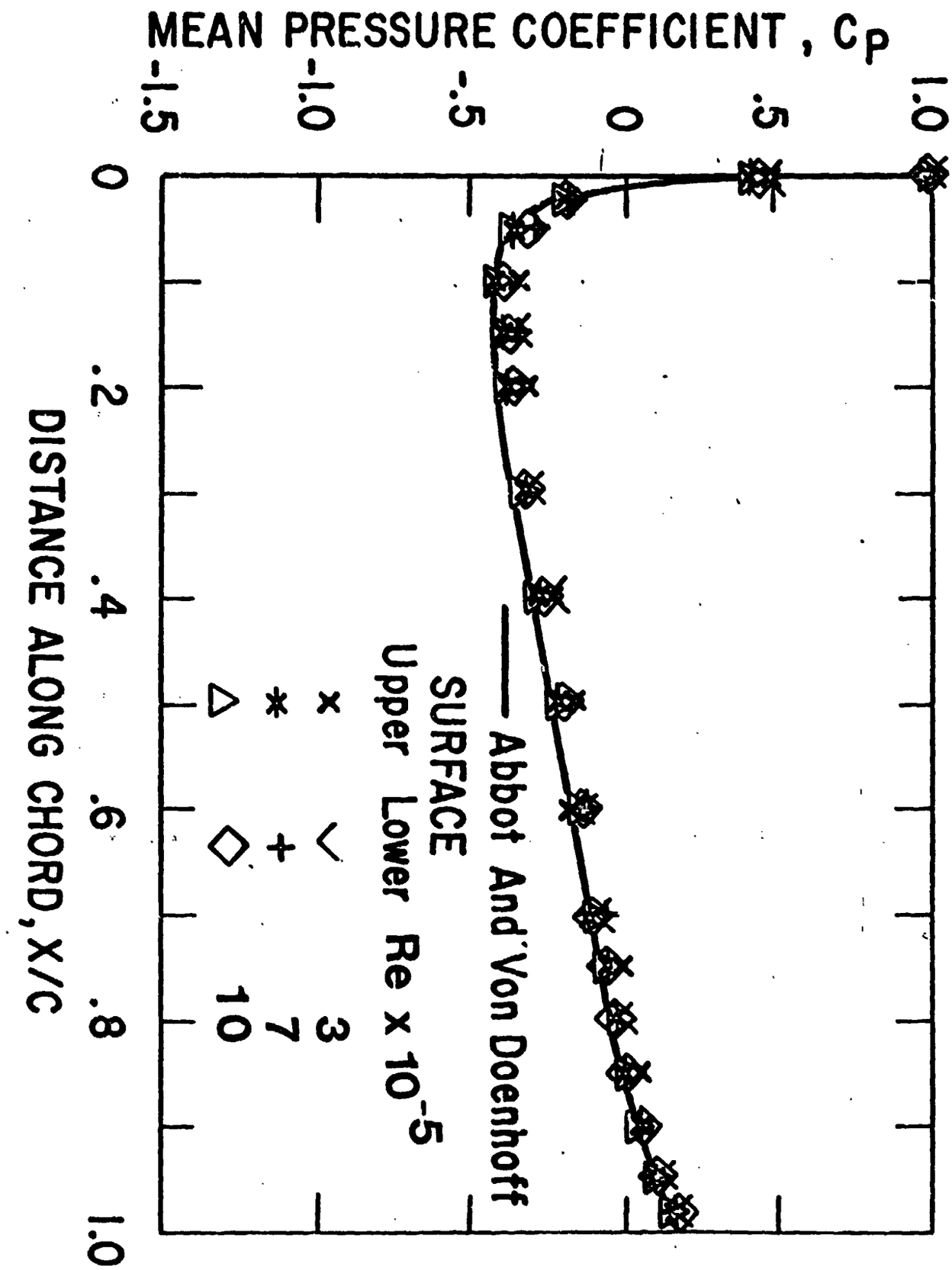
MEAN PRESSURE COEFFICIENT , C_p
-1.5
-1.0
-.5
0
.5
1.0
0
.2
.4
.6
.8
1.0
DISTANCE ALONG CHORD, X/C
Abbot And Von Doenhoff
SURFACE
Upper Lower Re x 10^{-5}
3
7
10

FIGURE 3

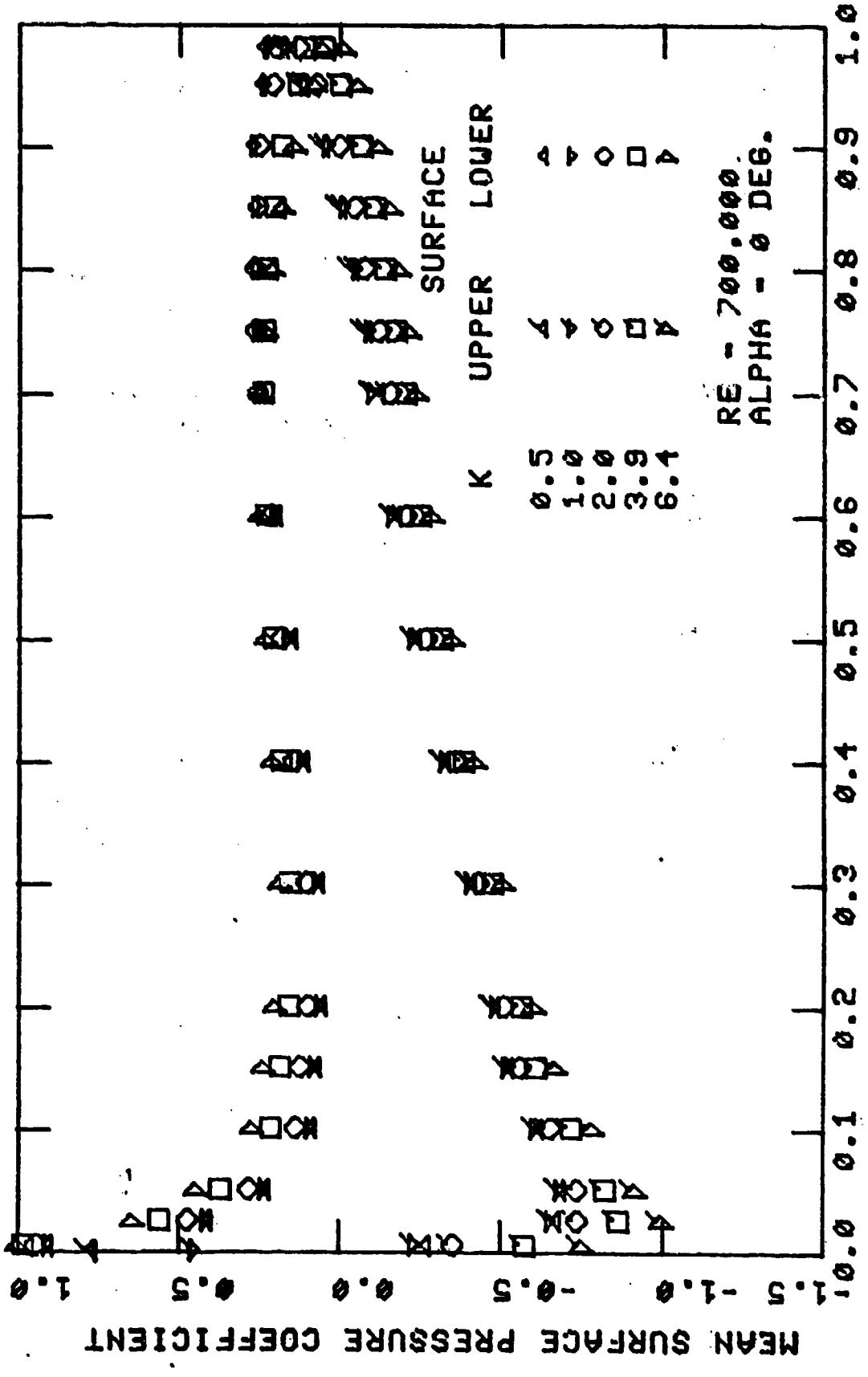
MEAN SURFACE PRESSURE COEFFICIENT
1.5
1.0
0.5
0.0
-0.5
-1.0
1.0
0.9
0.8
0.7
0.6
0.5
0.4
0.3
0.2
0.1
0.0
DISTANCE ALONG CHORD, X/C
SURFACE
UPPER
LOWER
K
0.5
1.0
2.0
3.9
6.4
RE = 700,000.
ALPHA = 0 DEG.

FIGURE 4

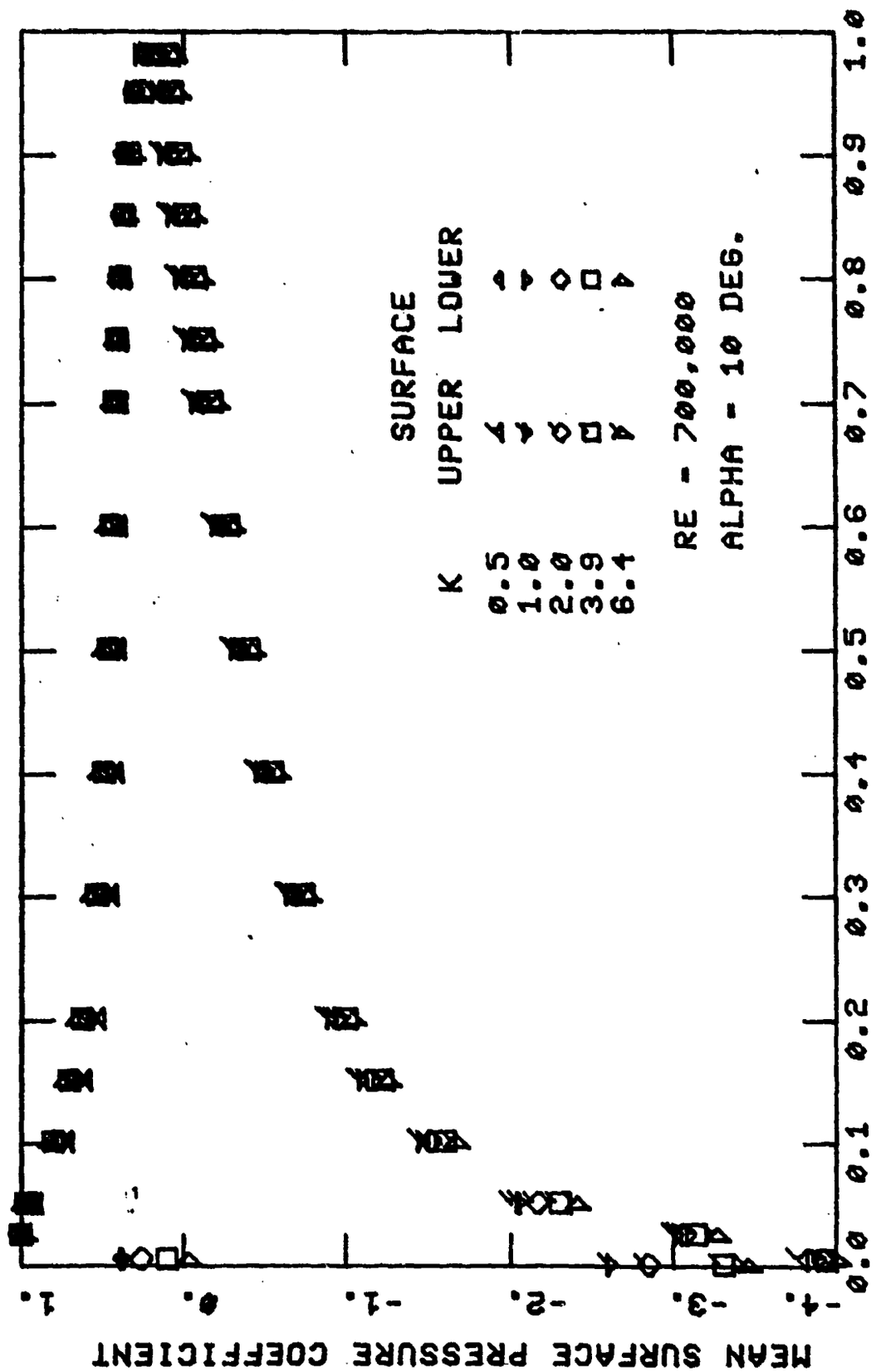
MEAN SURFACE PRESSURE COEFFICIENT
1.
0.
-1.
-2.
-3.
-4.
0.0
0.1
0.2
0.3
0.4
0.5
0.6
0.7
0.8
0.9
1.0
DISTANCE ALONG CHORD, X/C
SURFACE
K UPPER LOWER
0.5
1.0
2.0
3.9
6.4
RE = 700,000
ALPHA = 10 DEG.

FIGURE 5

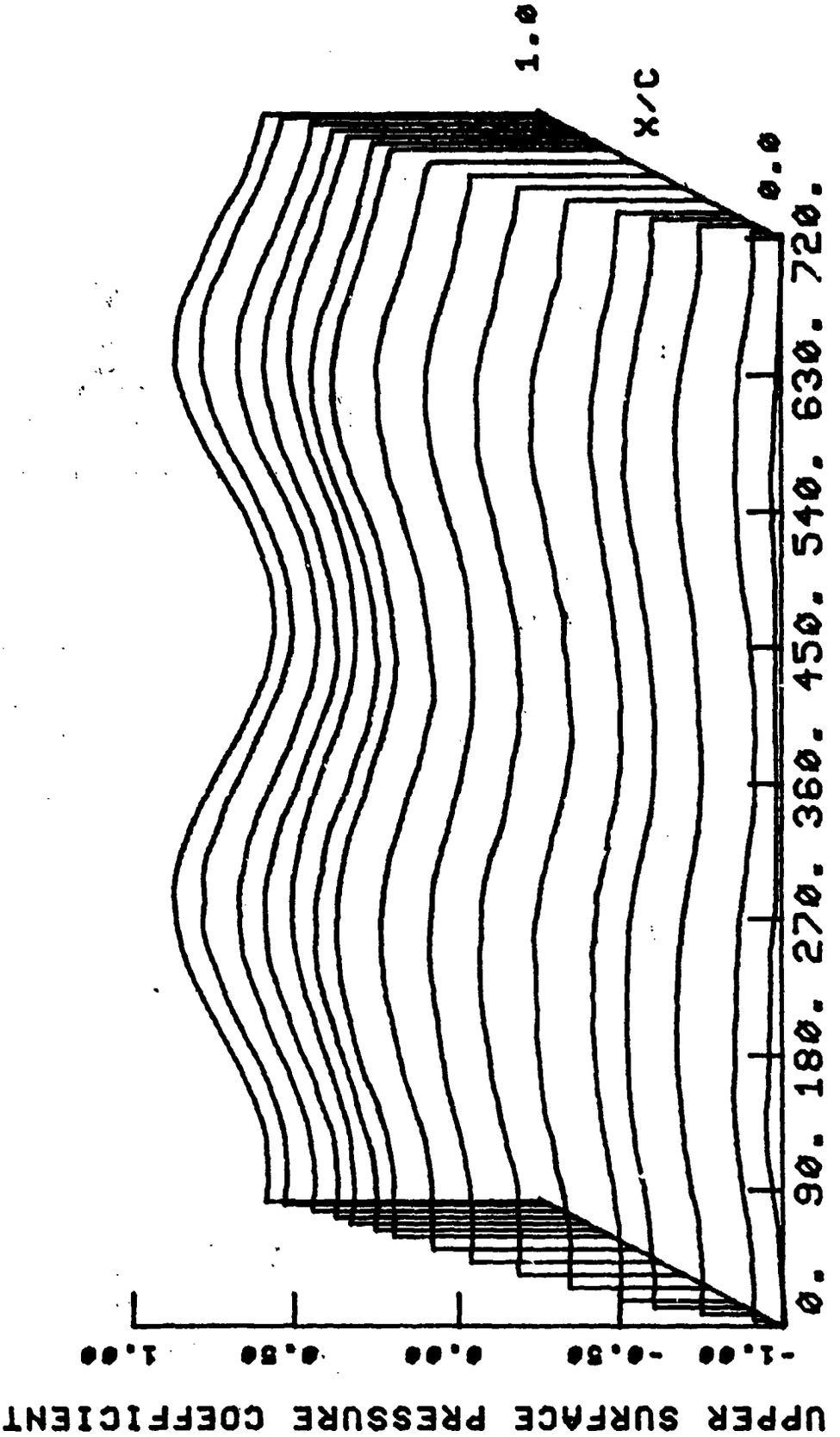
UPPER SURFACE PRESSURE COEFFICIENT
-1.00
-0.50
0.00
0.50
1.00
X/C
1.0
0.0
0. 90. 180. 270. 360. 450. 540. 630. 720.
TIME IN DEGREES OF PHASE K-6.4.ALPHA- 0.

FIGURE 6

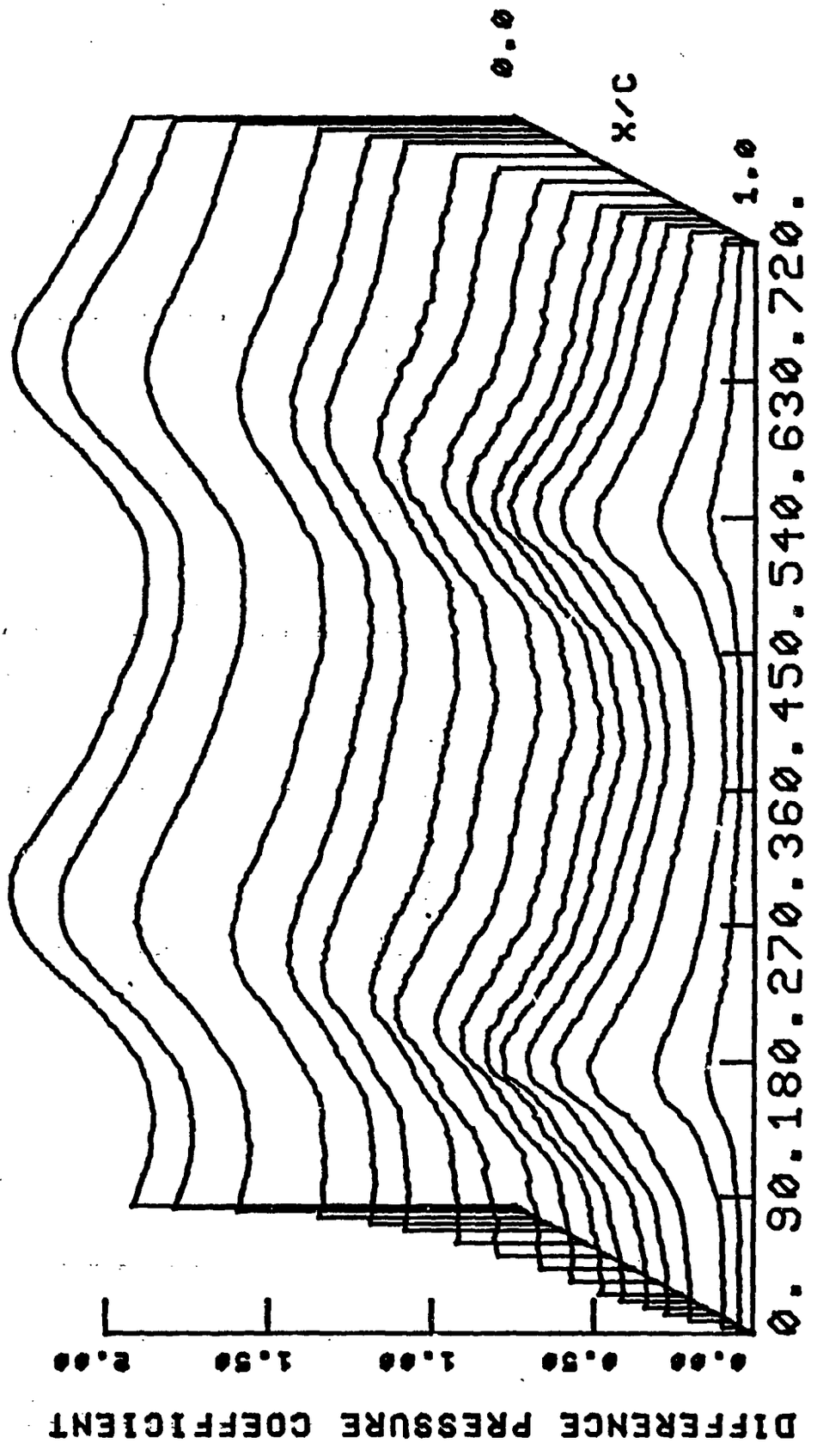
DIFFERENCE PRESSURE COEFFICIENT
0.00
0.50
1.00
1.50
2.00
0. 90. 180. 270. 360. 450. 540. 630. 720.
TIME IN DEGREES OF PHASE, K= 1.0.
X/C
0.0
1.0

FIGURE 7

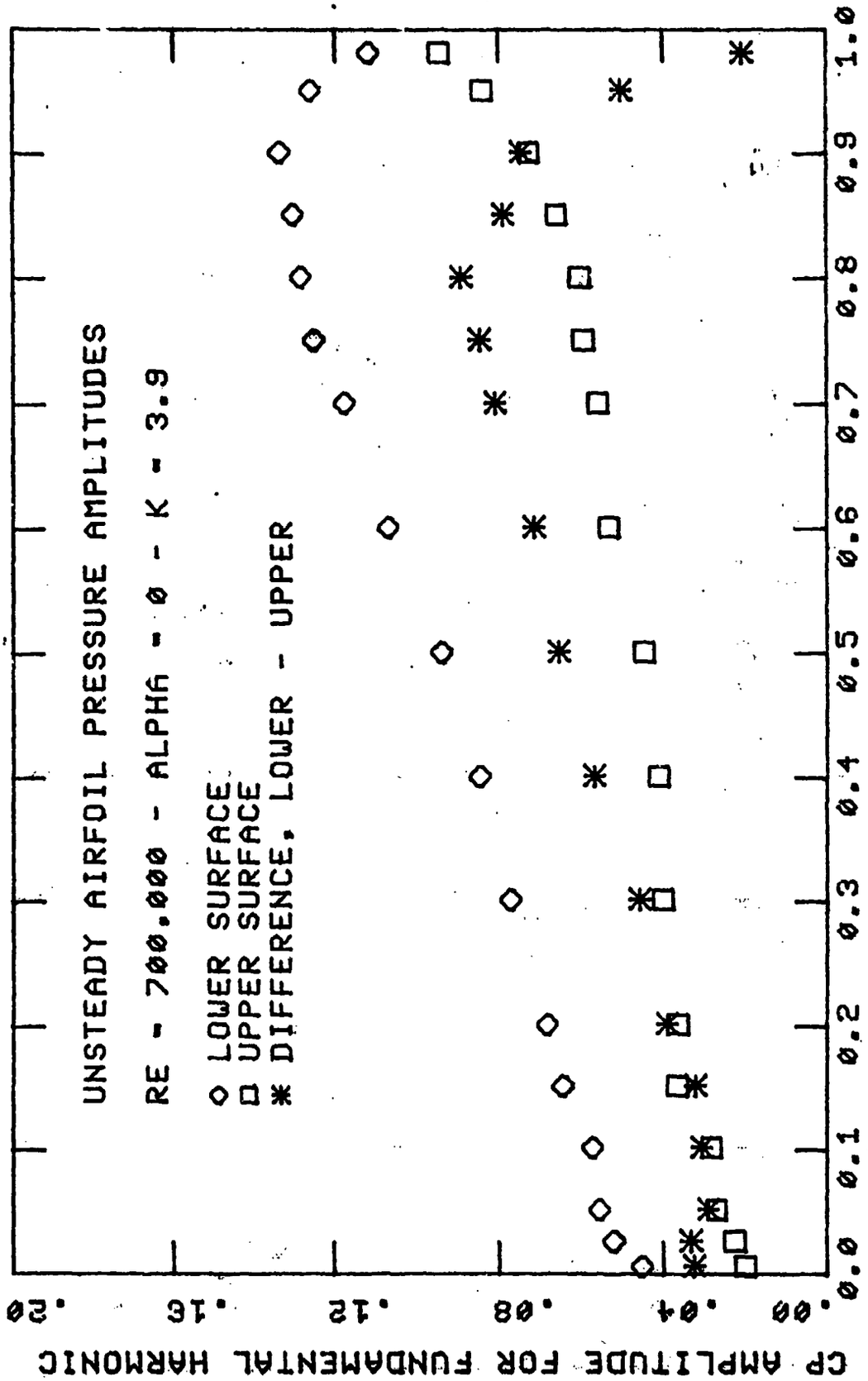
UNSTEADY AIRFOIL PRESSURE AMPLITUDES
RE = 700,000 - ALPHA = 0 - K = 3.9
◇ LOWER SURFACE
□ UPPER SURFACE
✱ DIFFERENCE, LOWER - UPPER
CP AMPLITUDE FOR FUNDAMENTAL HARMONIC
.00
.04
.08
.12
.16
.20
0.0
0.1
0.2
0.3
0.4
0.5
0.6
0.7
0.8
0.9
1.0
DISTANCE ALONG CHORD, X/C

FIGURE 8

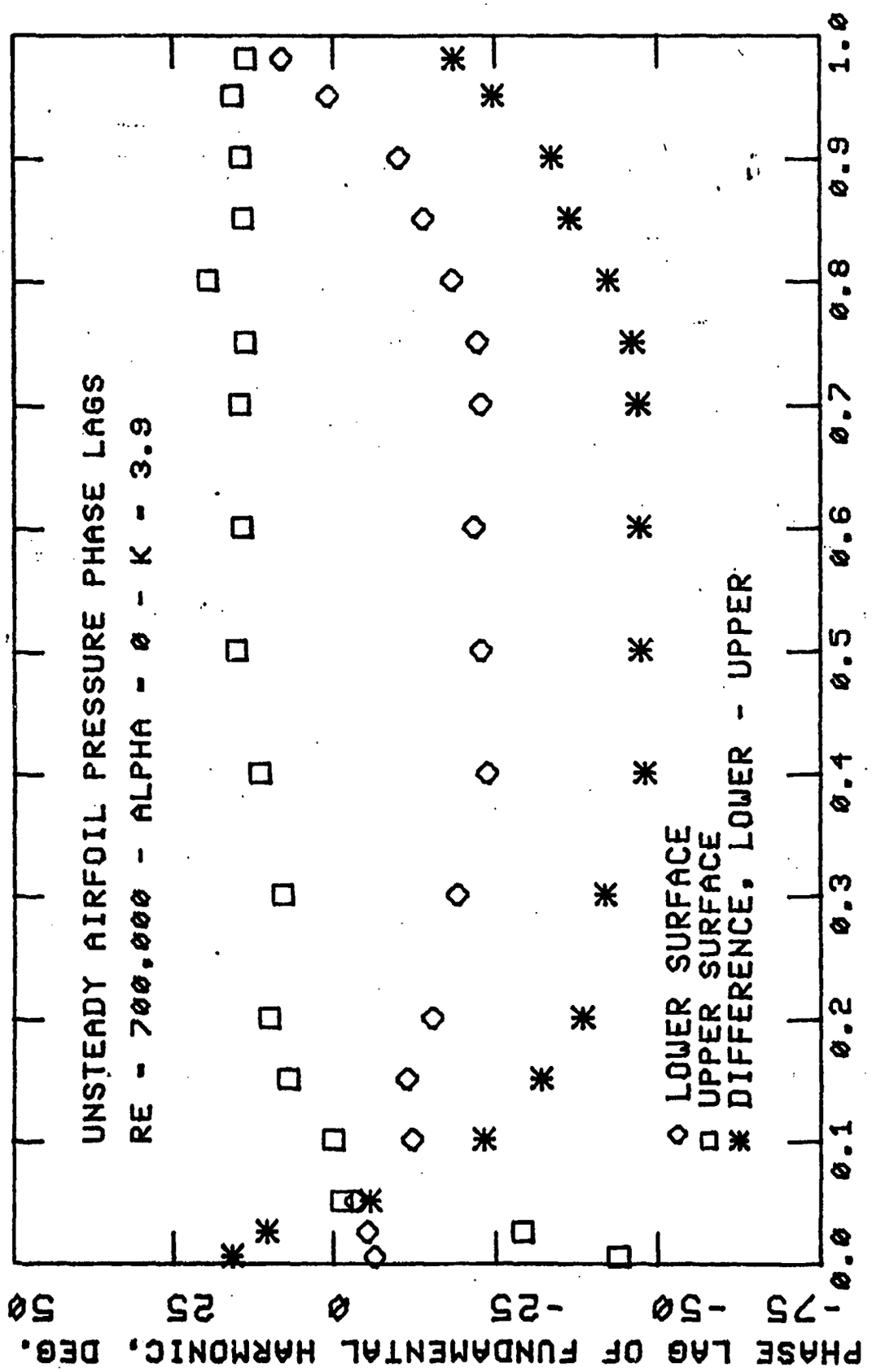
UNSTEADY AIRFOIL PRESSURE PHASE LAGS
RE = 700,000 - ALPHA = 0 - K = 3.9
LOWER SURFACE
UPPER SURFACE
DIFFERENCE, LOWER - UPPER
PHASE LAG OF FUNDAMENTAL HARMONIC, DEG.
50
25
0
-25
-50
-75
DISTANCE ALONG CHORD, X/C
0.0
0.1
0.2
0.3
0.4
0.5
0.6
0.7
0.8
0.9
1.0

FIGURE 9

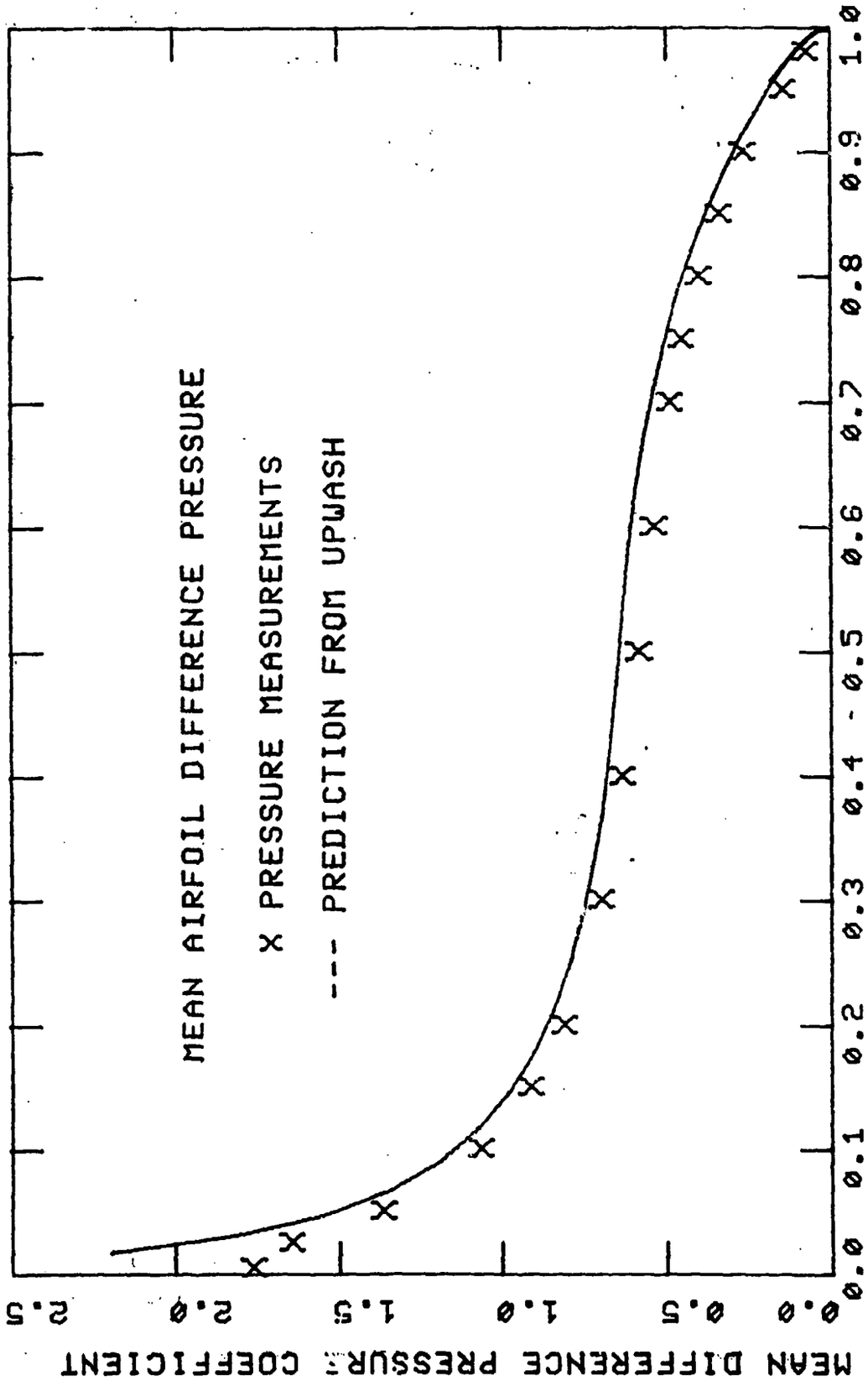
MEAN AIRFOIL DIFFERENCE PRESSURE
X PRESSURE MEASUREMENTS
--- PREDICTION FROM UPWASH
MEAN DIFFERENCE PRESSURE COEFFICIENT
0.0
0.5
1.0
1.5
2.0
2.5
0.0
0.1
0.2
0.3
0.4
0.5
0.6
0.7
0.8
0.9
1.0
DISTANCE, X/C - K-6.4, ALPHA-0, RE-700,000 APR81

FIGURE 10

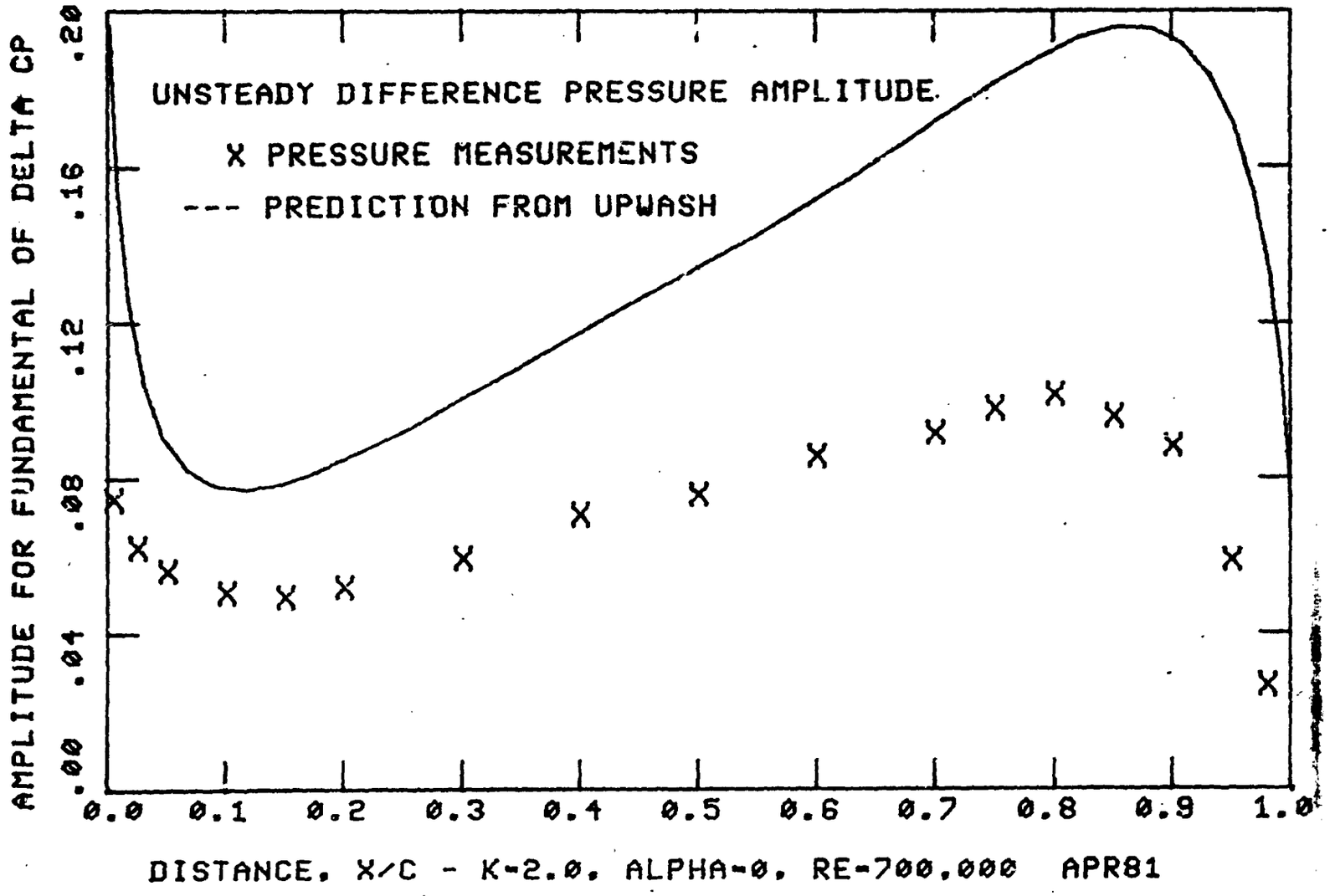
UNSTEADY DIFFERENCE PRESSURE AMPLITUDE
X PRESSURE MEASUREMENTS
--- PREDICTION FROM UPWASH
AMPLITUDE FOR FUNDAMENTAL OF DELTA CP
.00
.04
.08
.12
.16
.20
0.0
0.1
0.2
0.3
0.4
0.5
0.6
0.7
0.8
0.9
1.0
DISTANCE, X/C - K-2.0, ALPHA-0, RE-700,000 APR81

FIGURE 11

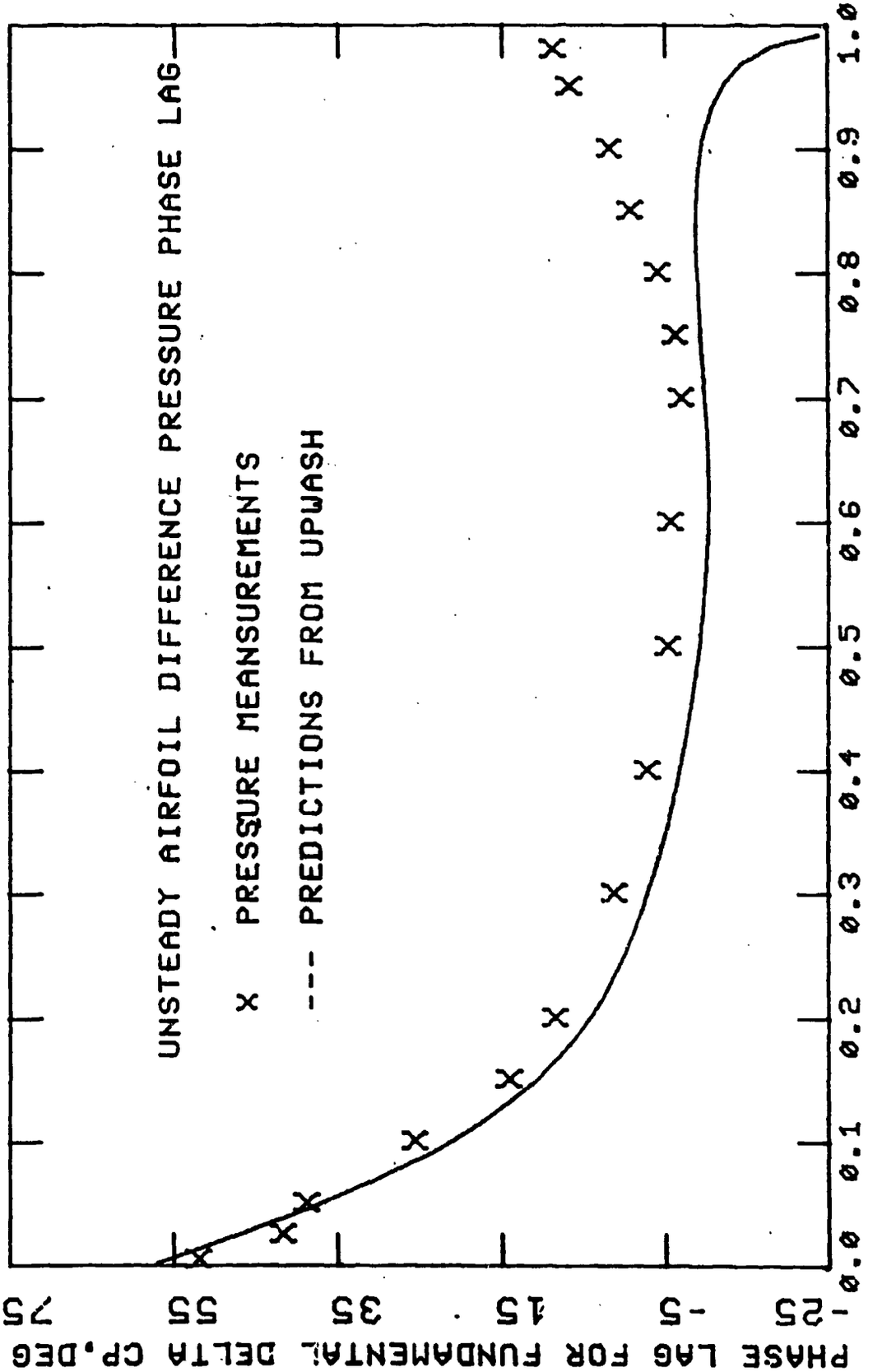
UNSTEADY AIRFOIL DIFFERENCE PRESSURE PHASE LAG
X PRESSURE MEANSUREMENTS
--- PREDICTIONS FROM UPWASH
PHASE LAG FOR FUNDAMENTAL DELTA CP,DEG
-25
-5
15
35
55
75
0.0
0.1
0.2
0.3
0.4
0.5
0.6
0.7
0.8
0.9
1.0
DISTANCE, X/C - K=2.0, ALPHA=0, RE=700,000 APR81

FIGURE 12

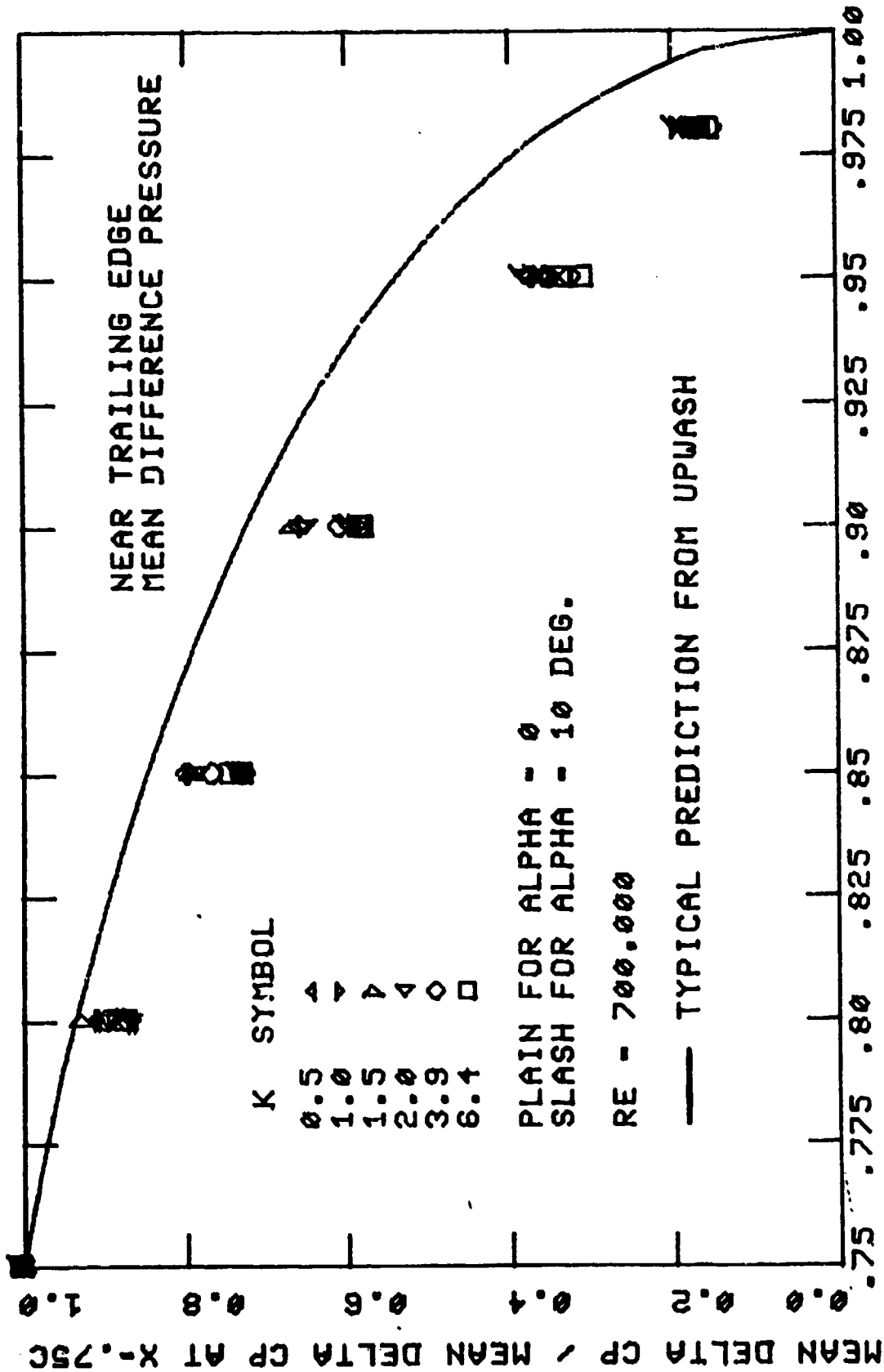
NEAR TRAILING EDGE
MEAN DIFFERENCE PRESSURE
K SYMBOL
0.5
1.0
1.5
2.0
3.9
6.4
PLAIN FOR ALPHA = 0
SLASH FOR ALPHA = 10 DEG.
RE = 700,000
TYPICAL PREDICTION FROM UPWASH
MEAN DELTA CP / MEAN DELTA CP AT X=.75C
0.0
0.2
0.4
0.6
0.8
1.0
.75
.775
.80
.825
.85
.875
.90
.925
.95
.975
1.00
DISTANCE ALONG AIRFOIL CHORD, X/C

FIGURE 13

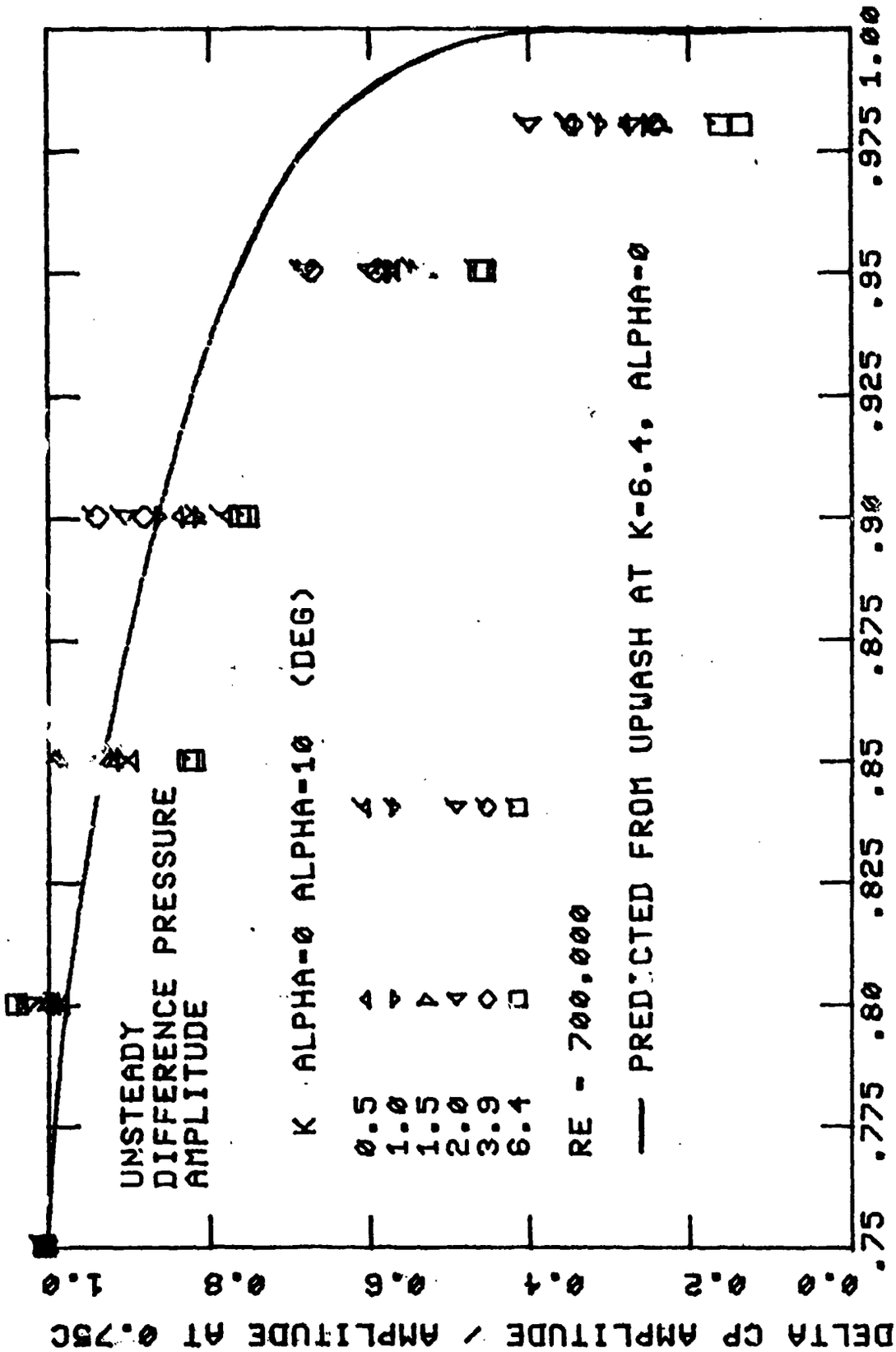
DELTA CP AMPLITUDE / AMPLITUDE AT 0.75C
0.0
0.2
0.4
0.6
0.8
1.0
.75
.775
.80
.825
.85
.875
.90
.925
.95
.975
1.00
DISTANCE ALONG AIRFOIL CHORD, X/C
UNSTEADY DIFFERENCE PRESSURE AMPLITUDE
K ALPHA-0 ALPHA-10 (DEG)
0.5
1.0
1.5
2.0
3.9
6.4
RE - 700,000
PREDICTED FROM UPWASH AT K-6.4, ALPHA-0

FIGURE 14

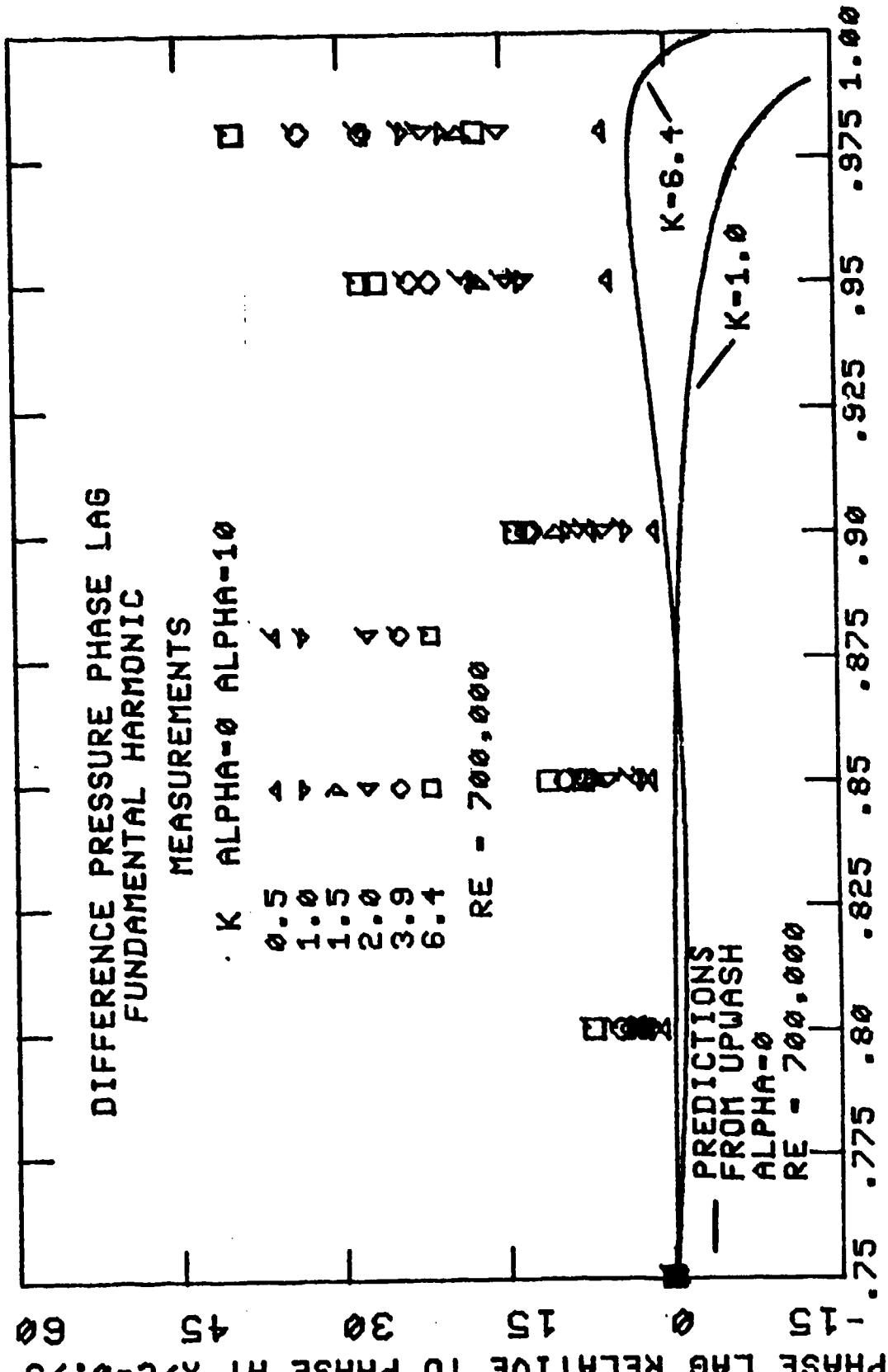
DIFFERENCE PRESSURE PHASE LAG
FUNDAMENTAL HARMONIC
MEASUREMENTS
K ALPHA-0 ALPHA-10
0.5
1.0
1.5
2.0
3.9
6.4
RE = 700,000
PREDICTIONS
FROM UPWASH
ALPHA-0
RE = 700,000
K-6.4
K-1.0
PHASE LAG RELATIVE TO PHASE AT X/C-0.75
-15
0
15
30
45
60
.75
.775
.80
.825
.85
.875
.90
.925
.95
.975
1.00
DISTANCE ALONG AIRFOIL CHORD, X/C

FIGURE 15

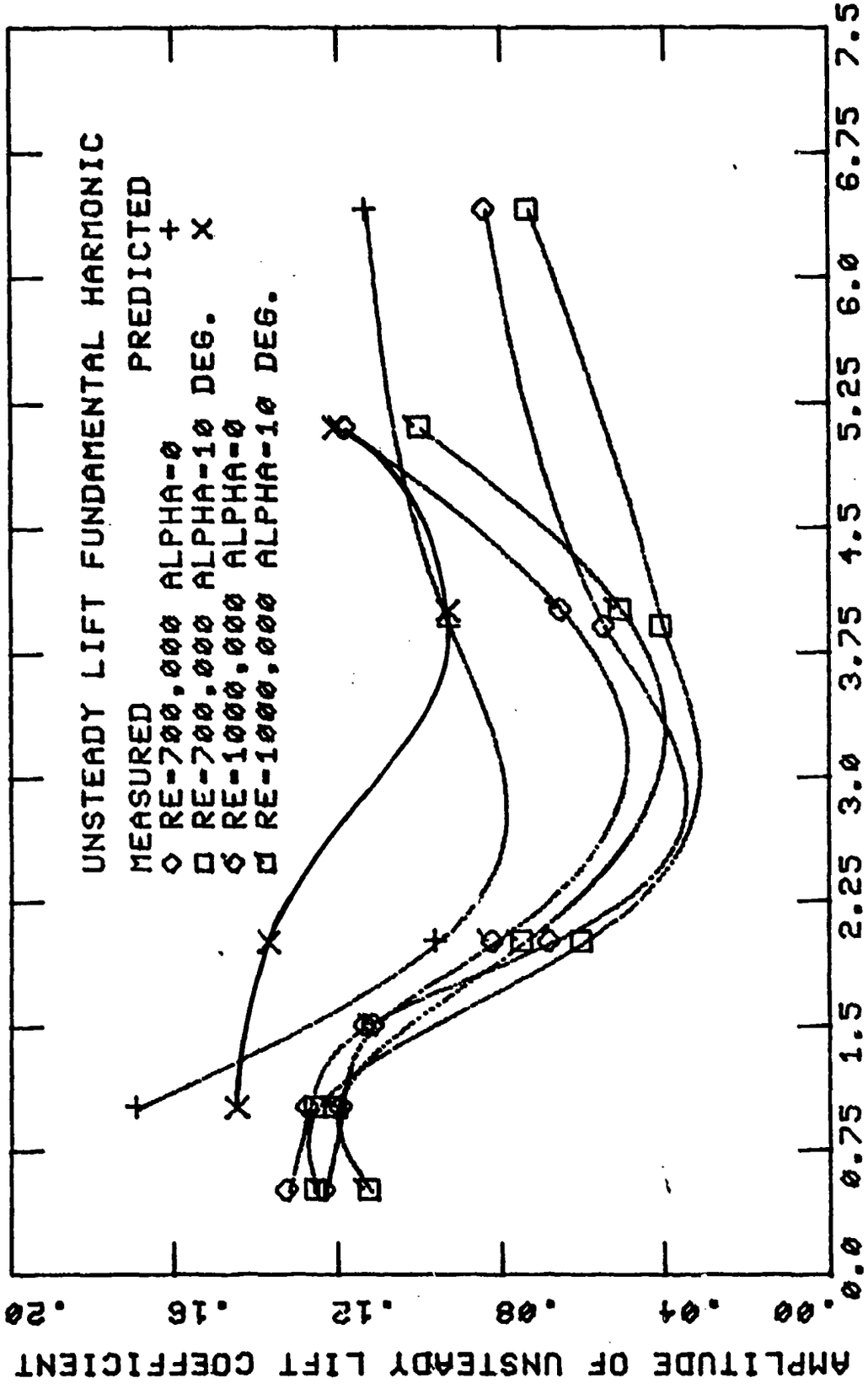
UNSTEADY LIFT FUNDAMENTAL HARMONIC
MEASURED
PREDICTED
◇ RE-700,000 ALPHA-0
□ RE-700,000 ALPHA-10 DEG.
◇ RE-1000,000 ALPHA-0
□ RE-1000,000 ALPHA-10 DEG.
AMPLITUDE OF UNSTEADY LIFT COEFFICIENT
.00
.04
.08
.12
.16
.20
0.0
0.75
1.5
2.25
3.0
3.75
4.5
5.25
6.0
6.75
7.5
REDUCED FREQUENCY, K

FIGURE 16

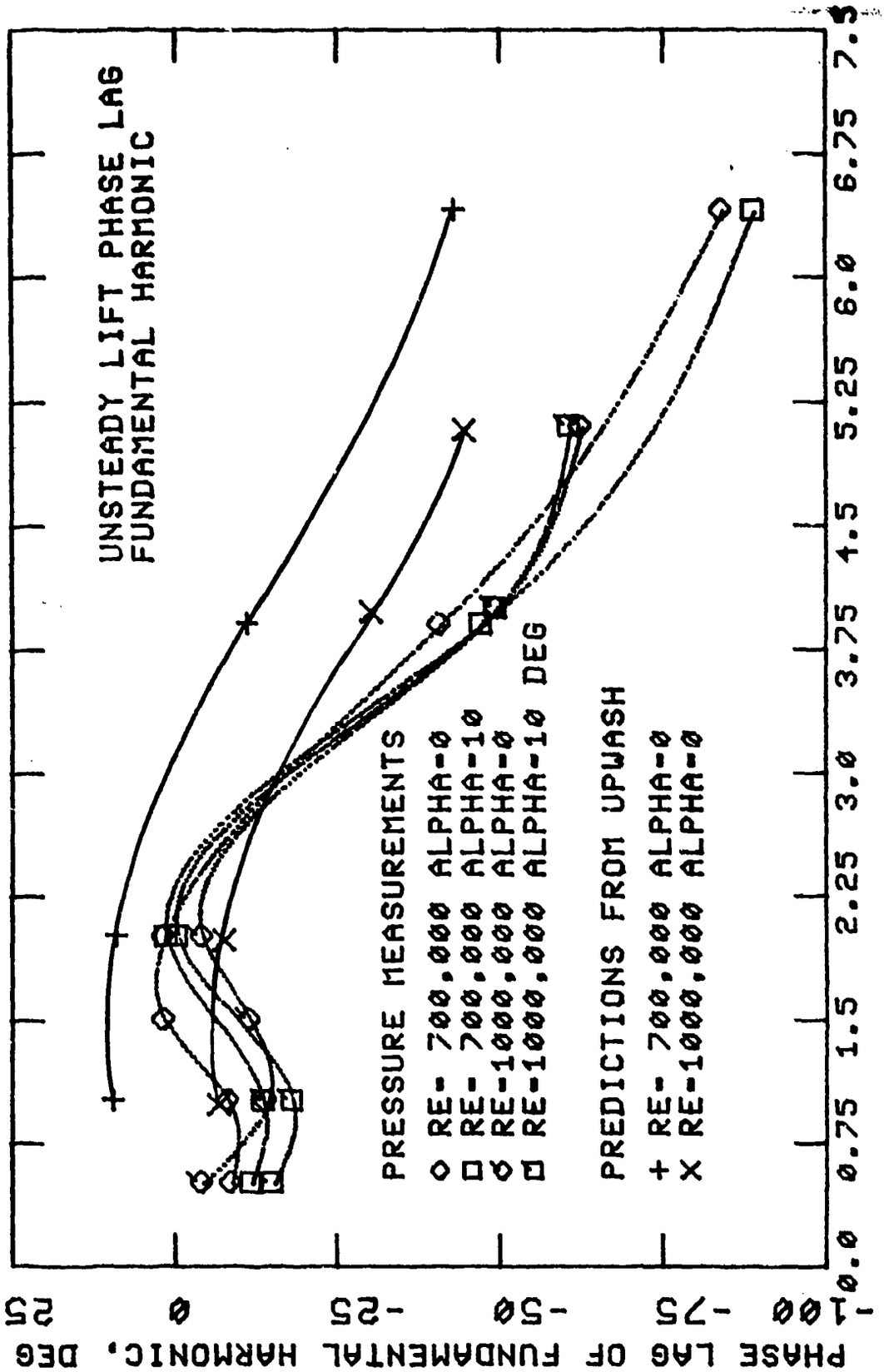
UNSTEADY LIFT PHASE LAG
FUNDAMENTAL HARMONIC
PRESSURE MEASUREMENTS
◇ RE- 700,000 ALPHA-0
□ RE- 700,000 ALPHA-10
◇ RE-1000,000 ALPHA-0
□ RE-1000,000 ALPHA-10 DEG
PREDICTIONS FROM UPWASH
+ RE- 700,000 ALPHA-0
× RE-1000,000 ALPHA-0
PHASE LAG OF FUNDAMENTAL HARMONIC, DEG
25
0
-25
-50
-75
-100
0.0
0.75
1.5
2.25
3.0
3.75
4.5
5.25
6.0
6.75
7.5
REDUCED FREQUENCY, K

FIGURE 17

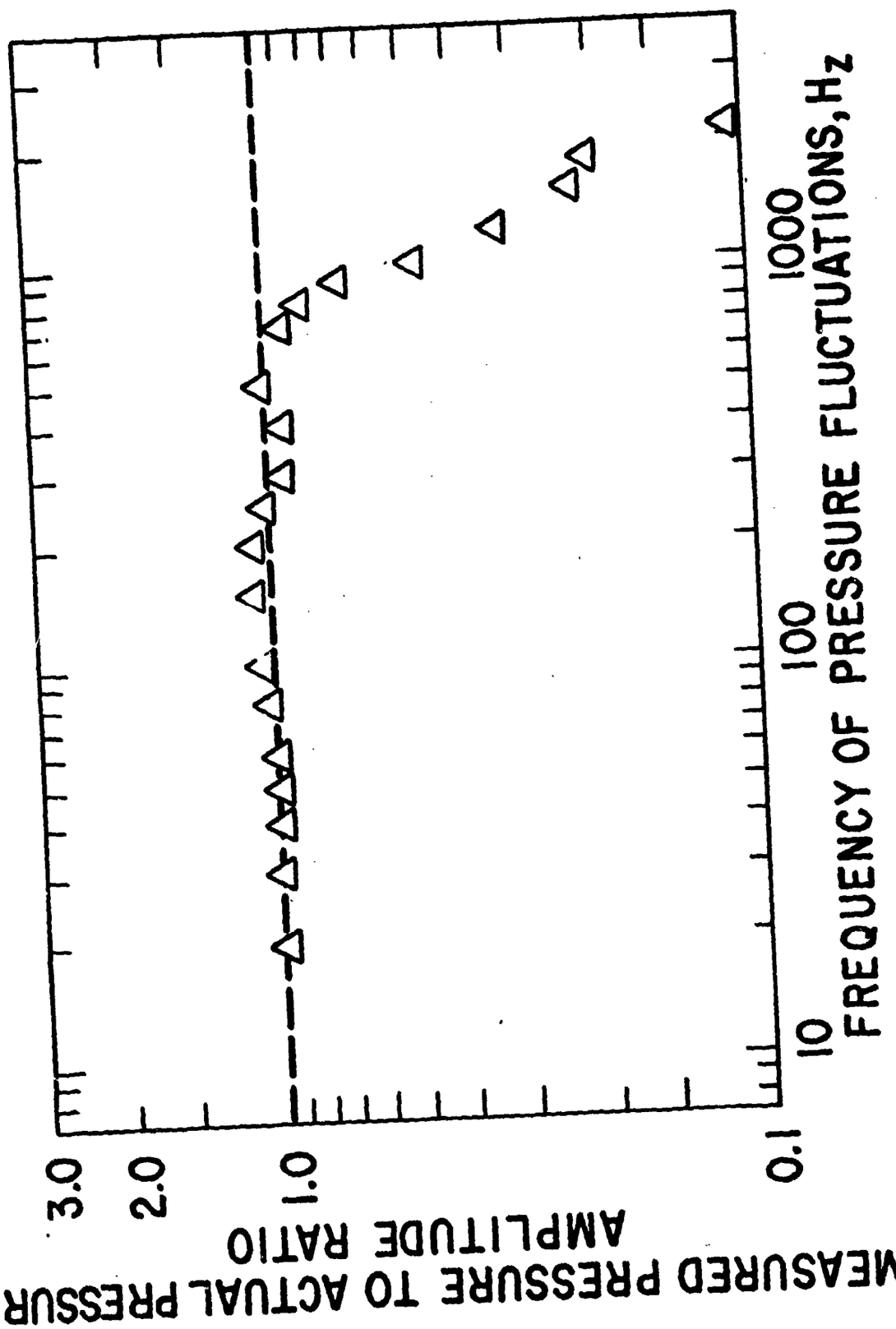
MEASURED PRESSURE TO ACTUAL PRESSURE, AMPLITUDE RATIO
3.0
2.0
1.0
0.1
10
100
1000
FREQUENCY OF PRESSURE FLUCTUATIONS, Hz

FIGURE A1

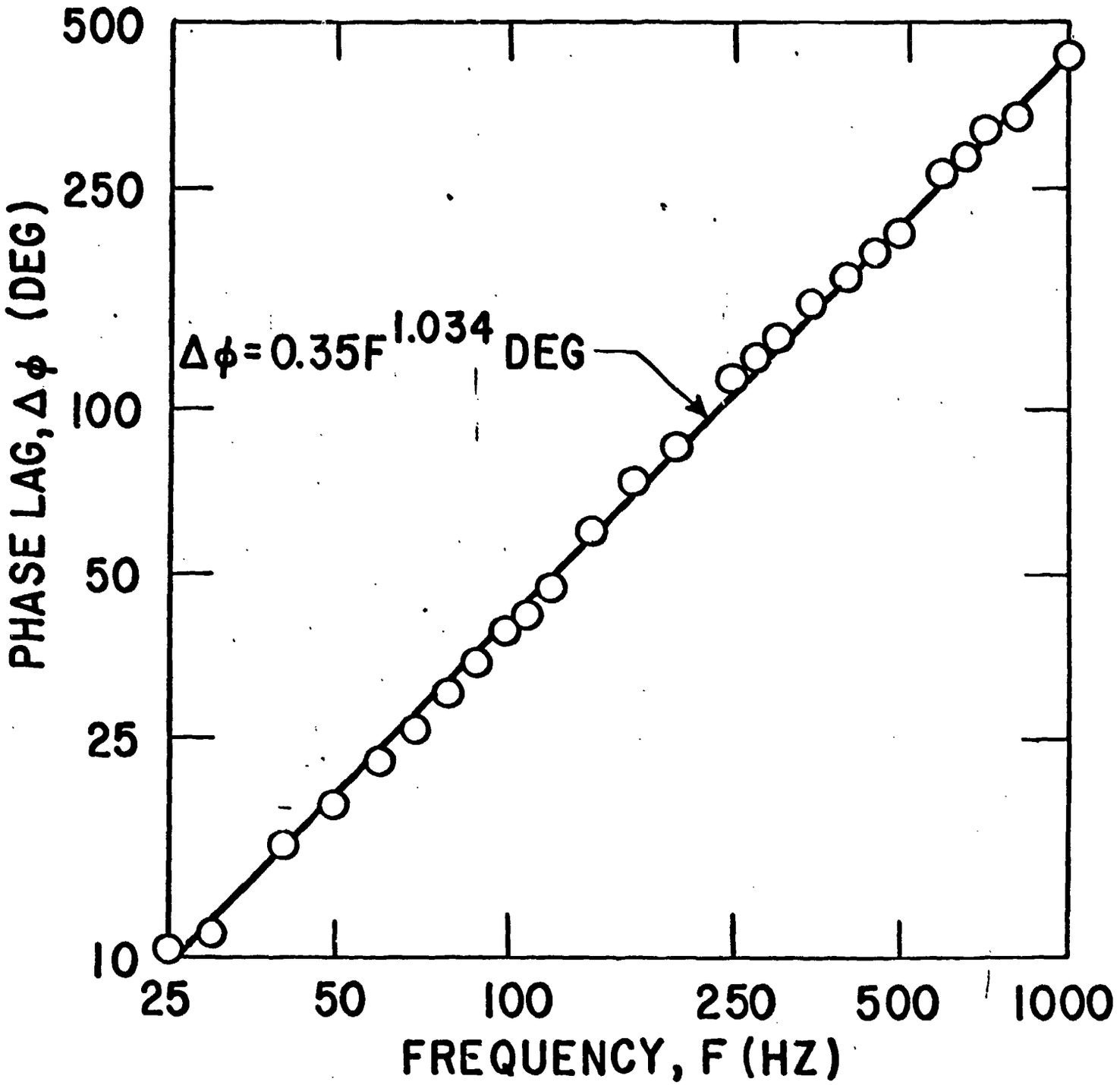
500
250
100
50
25
10
PHASE LAG, Δφ (DEG)
Δφ = 0.35F^1.034 DEG
25
50
100
250
500
1000
FREQUENCY, F (HZ)

FIGURE A2